

Physicochemical Characterisation and Industrial Applications of Umuchieze Mined Kaolin Clay

Beneth C. Chukwudi, Briggs M. O. Ogunedo*

Department of Mechanical Engineering, Imo State University, Owerri, Nigeria

*Corresponding Author: Briggs M. O. Ogunedo

ABSTRACT

This study comprehensively characterizes the physicochemical properties of Umuchieze kaolin clay using a suite of analytical techniques, including FTIR, SEM/EDS, TGA, and BET analyses. The FTIR results confirm a well-developed kaolinite structure, with distinct silicate framework vibrations in the low-frequency region ($640\text{--}1163\text{ cm}^{-1}$) and multiple O–H stretching bands in the high-frequency region ($3620\text{--}3691\text{ cm}^{-1}$), indicative of a highly ordered silicate matrix with variable hydroxyl environments. SEM/EDS analysis reveals a composition dominated by oxygen, silicon, and aluminium, consistent with the ideal kaolinite formula, while trace elements such as carbon, titanium, and iron are present at low levels. TGA demonstrates initial mass loss due to adsorbed water below $100\text{ }^{\circ}\text{C}$, stability up to $320\text{ }^{\circ}\text{C}$, and dehydroxylation peaking at $480\text{ }^{\circ}\text{C}$, after which a thermally stable metakaolin phase is formed. BET analysis indicates a moderate surface area ($\sim 23.76\text{ m}^2/\text{g}$) and an average pore diameter of $\sim 25\text{ nm}$, confirming a predominantly mesoporous structure. These findings underscore the material's potential for high-quality paper production, environmental remediation, adsorption processes, and catalytic applications in oil and gas processes. Further studies are recommended to optimize surface modification and beneficiation techniques, thereby enhancing its performance in these advanced industrial applications.

KEYWORDS: Kaolin, Kaolinite, metakaolin, dehydroxylation, Adsorption, paper production, physicochemical properties.

1. INTRODUCTION

Kaolin clay is a versatile industrial material renowned for its unique physico-chemical properties, which have led to its widespread use in ceramics, paper, rubber, cosmetics, pharmaceuticals, and environmental remediation [1–3]. Derived from the weathering of feldspathic rocks, kaolin primarily consists of kaolinite an aluminosilicate mineral with the chemical formula $\text{Al}_2\text{Si}_2\text{O}_5(\text{OH})_4$ and a characteristic two-dimensional layered structure [4]. It has a 2:1 (T-O) structure, meaning it is composed of alternating tetrahedral (T) silica and octahedral (O) alumina sheets. Kaolin consists of stacked layers, each made up of two fundamental sheets. The T Sheet made up of SiO_4 tetrahedra linked together in a

hexagonal arrangement. As seen in figure 1, each tetrahedron shares three oxygen atoms with adjacent tetrahedra, while the fourth oxygen bonds with aluminium in the octahedral sheet. The O Sheet is composed of Al_2O_6 octahedra, where aluminium (Al^{3+}) is surrounded by six hydroxyl groups (OH^-) or oxygen atoms. This sheet forms a gibbsite-like layer that interacts with the tetrahedral silica layer above it. As depicted in figure 1, the tetrahedral and octahedral sheets are linked together via shared oxygen atoms, forming one structural unit. Multiple units are stacked together through hydrogen bonding, creating a non-swelling structure and platy morphology characteristic of kaolin.

How to cite this paper: Beneth C. Chukwudi | Briggs M. O. Ogunedo "Physicochemical Characterisation and Industrial Applications of Umuchieze Mined Kaolin Clay" Published in International

Journal of Trend in Scientific Research and Development (ijtsrd), ISSN: 2456-6470, Volume-9 | Issue-4, August 2025, pp.1004-1015,

URL: www.ijtsrd.com/papers/ijtsrd97369.pdf



Copyright © 2025 by author (s) and International Journal of Trend in Scientific Research and Development Journal. This is an Open Access article distributed under the terms of the Creative Commons Attribution License (CC BY 4.0) (<http://creativecommons.org/licenses/by/4.0>)



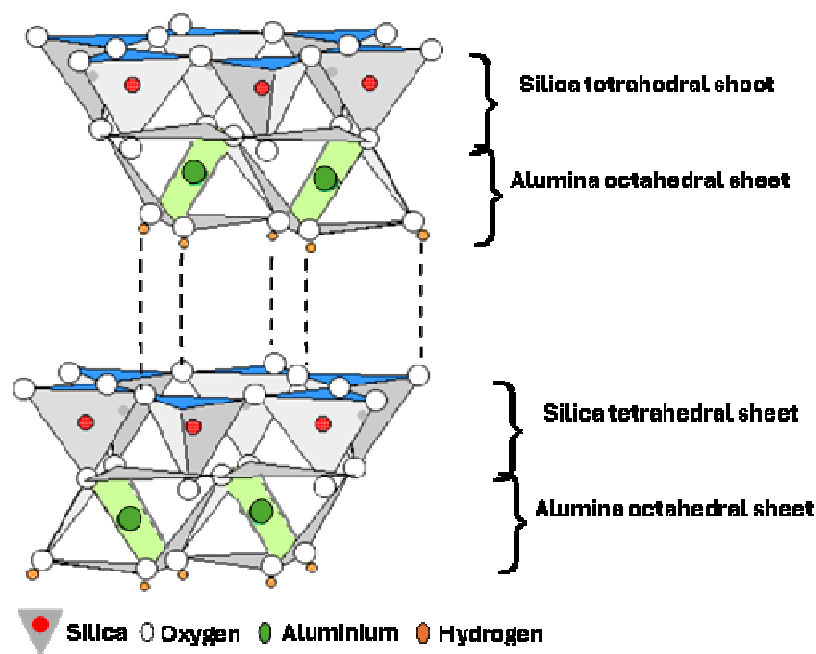


Fig. 1: Illustration of a kaolin structure.

Kaolin high whiteness, low abrasiveness, and good thermal stability have been instrumental in ensuring product quality in various industries, while its chemical inertness and high cation exchange capacity further enhance its applicability in environmental cleanup processes [6,7].

Despite the extensive global utilization of kaolin, the physico-chemical properties of this material can vary significantly with the geological origin of the deposits, necessitating thorough characterization to optimize its industrial use [8]. Advanced analytical techniques such as Fourier-transform infrared spectroscopy (FTIR) [9,10], scanning electron microscopy (SEM) [11], Brunauer–Emmett–Teller (BET) analysis [6], and thermogravimetric analysis (TGA) [12] are critical for elucidating the mineralogical composition, structural features, thermal behaviour, and chemical makeup of kaolin clays. Such comprehensive studies not only enhance the fundamental understanding of kaolin but also facilitate the development of targeted beneficiation and processing strategies tailored to specific industrial applications.

Nigeria is endowed with abundant kaolin reserves as shown in the mineral resources map in figure 2 [13].

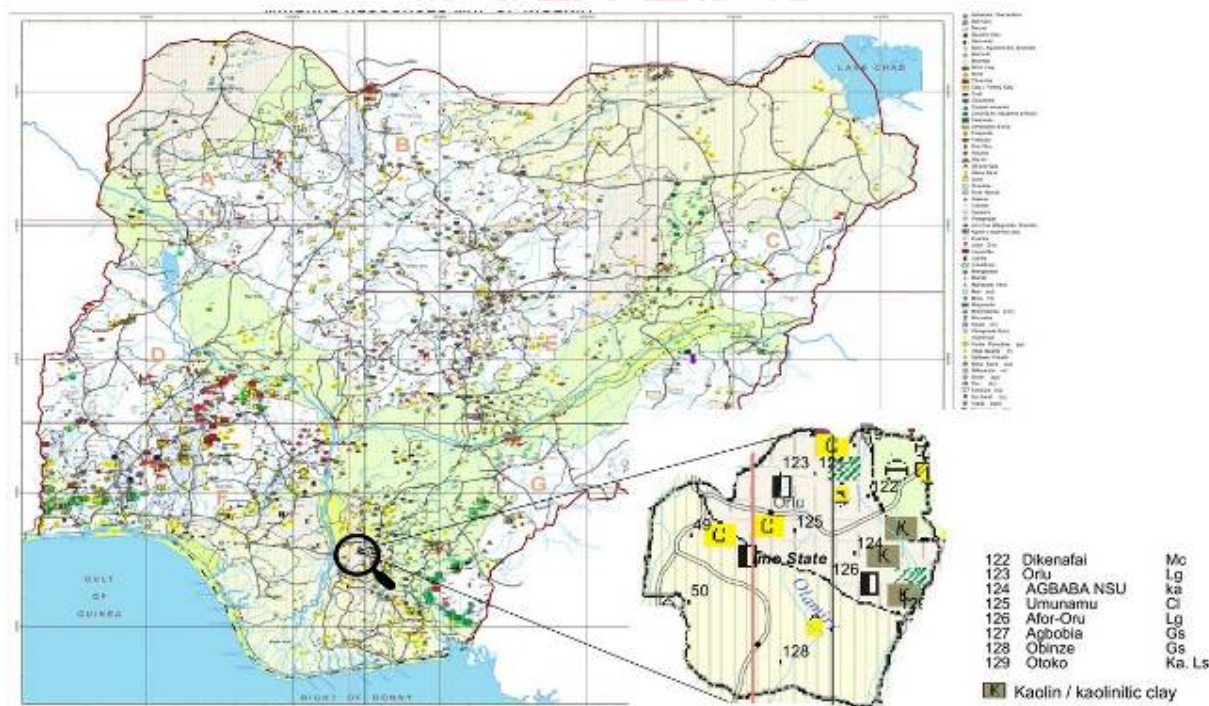


Fig. 2: Mineral resources map of Nigeria showing location of kaolin deposits in Imo state [13].

Reports exist on the characterisation of some of these Kaolin reserves in places such as Ijero-Ekiti, Ikere-Ekiti, Isan-Ekiti, Abusoro and Odigbo [14], Auchi [15], Alkalari [16], Nsu [17], Eha-Ndiagu [18], Lakiri [19], Kaoje [20], Ifon [21], Avutu Obowo [22], Akoko [23], Umuoike Obowo [24], Kankara [25], Ijero-Ekiti, Ode-Irele, and Iwo [26], Nsu, Onuiyi Obowo, Nkumeato, Oboro, Kutigi, and Afuze [27], Okpella [28]. These studies present a significant yet underexploited resource, with many deposits remaining inadequately characterized. One such deposit is located in Umuchieze in Ihitteafoukwu Ekwerazu Ahiazu Mbaise of Imo state, in the southeastern region of Nigeria. Although the region is recognized for its rich mineral endowment, detailed investigations into the properties and potential industrial applications of Umuchieze kaolin is yet to be studied and is not captured in the mineral resources map of Nigeria as shown in figure 1. Addressing this gap, the present study aims to provide a detailed physico-chemical characterization of kaolin clay from the Umuchieze deposit. Through the application of advanced analytical methods, the study seeks to delineate the material's mineralogical and structural characteristics, thermal stability, and chemical composition, thereby assessing its suitability for a range of industrial applications.

The outcomes of this research are anticipated to offer critical insights into the performance of Umuchieze kaolin, potentially bolstering local industrial processes and reducing reliance on imported raw materials. Furthermore, the study underscores the broader significance of characterizing indigenous mineral resources in developing countries, contributing to sustainable economic growth and the advancement of environmentally compatible technologies in both local and international markets.

2. Materials and Methods

2.1. Sample Collection and Preparation

Kaolin clay samples were collected from various locations within the Umuchieze mining site to ensure representativeness. The samples were air-dried to remove moisture, ground using a mortar and pestle, and sieved to achieve a uniform particle size distribution (less than 75 μm).

2.2. Fourier Transform Infrared Spectroscopy (FTIR)

FTIR analysis was performed to identify functional groups, and chemical bonds present in the kaolin clay. Spectra were recorded in the range of 4000–600 cm^{-1} using a Nicolet Avatar 360 FTIR spectrometer at a resolution of 4 cm^{-1} , with 50 scans per measurement in triplicates. Each spectrum was acquired by subtracting the background from the original spectrum.

2.3. Scanning Electron Microscopy (SEM) and Energy Dispersive Spectroscopy (EDS)

The surface morphology and elemental composition of the samples were characterized using a Carl Zeiss evo10LS-EDAX scanning electron microscope equipped with energy-dispersive spectroscopy (EDS). Prior to imaging, the samples were sputter-coated with a thin layer of gold to enhance conductivity. SEM micrographs were acquired at magnifications ranging from 500 \times to 5000 \times to elucidate the sample morphology, and subsequent EDS mapping provided semi-quantitative elemental analysis of the materials.

2.4. Thermogravimetric Analysis (TGA)

Thermal stability and compositional analysis were assessed using thermogravimetric analysis. Approximately 10 mg of the kaolin sample was placed in a platinum crucible and heated from room temperature to 800 $^{\circ}\text{C}$ at a rate of 10 $^{\circ}\text{C}/\text{min}$ under a nitrogen atmosphere. Weight loss data were recorded to identify phases such as dehydroxylation and other thermal events.

2.5. Pore structure analysis

The specific surface area, pore size distribution, and total pore volume of the kaolin samples were determined using BET analysis. Approximately 0.5 g of sample was degassed at 120 $^{\circ}\text{C}$ for 12 hours under vacuum before nitrogen adsorption-desorption measurements were carried out using a micromeritics Tristar 3000 V4.02 surface area analyser. The specific surface area (SBET) was determined by applying the Brunauer–Emmett–Teller (BET) method within the relative pressure range of 0.05–0.20 [31]. The total pore volume (V_p) was estimated from the amount of nitrogen adsorbed at a relative pressure (p/p_0) of 0.99. The pore size distribution and average pore diameter were derived using the Barrett–Joyner–Halenda (BJH) method [32].

3. Results and Discussion

3.1. FTIR result: The FTIR spectrum of the kaolin clay sample as shown in figure 3 exhibits several well-defined absorption bands that can be correlated with the vibrational modes of the mineral's structural constituents.

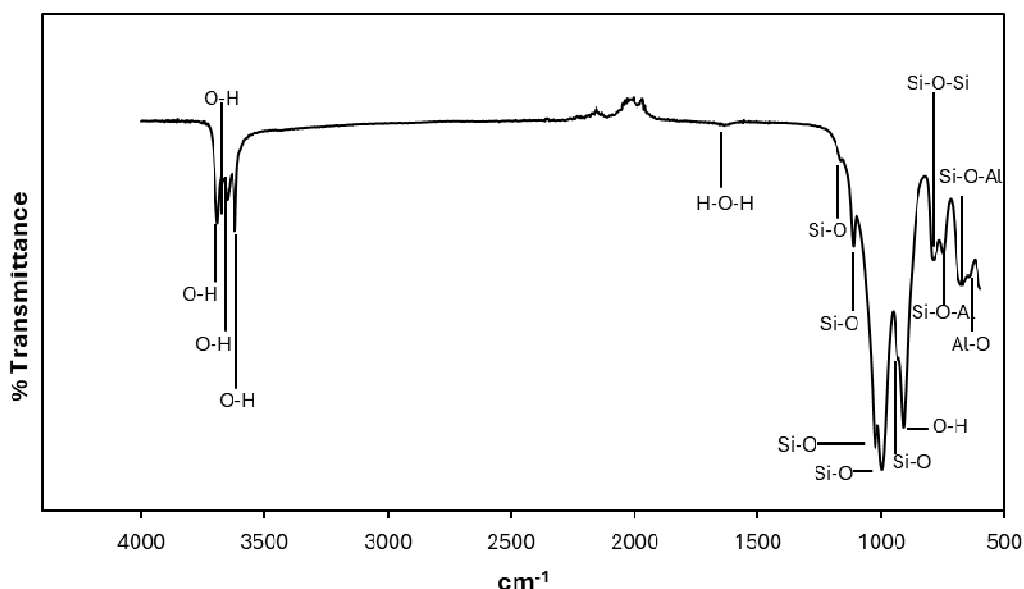


Fig. 3: FTIR spectrum of Umuchieze mined kaolin clay

In the low-frequency region ($640\text{--}1163\text{ cm}^{-1}$), the observed bands are primarily associated with the bending and stretching vibrations of the silicate framework and metal–oxygen bonds:

- 640 cm^{-1} : This band is attributed to Al–O bending vibrations, likely arising from distortions within the octahedral sheet.
- 675 cm^{-1} and 748 cm^{-1} : These absorptions are assigned to Si–O–Al bending vibrations, reflecting the interactions between the tetrahedral and octahedral layers of kaolinite.
- 790 cm^{-1} : This peak is indicative of the symmetric stretching of Si–O–Si bonds within the tetrahedral sheet.
- 908 cm^{-1} : Typically, a band in this region corresponds to the in-plane bending vibrations of inner hydroxyl groups.
- 935 cm^{-1} , 997 cm^{-1} , and 1026 cm^{-1} : These bands are associated with the stretching vibrations of Si–O bonds in the silicate framework, confirming the presence of a well-developed tetrahedral network.
- 1114 cm^{-1} and 1163 cm^{-1} : These peaks further corroborate the presence of Si–O stretching modes. The band at 1163 cm^{-1} may also suggest minor contributions from quartz impurities or reflect asymmetrical stretching vibrations characteristic of kaolinite.

The mid-frequency region includes the 1600 cm^{-1} band, which is commonly ascribed to the bending vibrations of adsorbed or structurally bound water molecules, a typical feature in clay minerals.

In the high-frequency region, four distinct bands are observed at 3620 cm^{-1} , 3651 cm^{-1} , 3670 cm^{-1} , and 3691 cm^{-1} . These bands are unambiguously assigned to the O–H stretching vibrations of the inner-surface hydroxyl groups within the kaolinite structure [29]. The presence of multiple peaks in this region reflects the existence of hydroxyl groups in different chemical environments, which is attributable to variations in hydrogen bonding and the local coordination geometry within the layered silicate structure. This also suggests a highly structured kaolinite mineral [30]. The consistency of the observed peak positions with those reported for typical kaolinite [10,29–32], confirms the mineral's characteristic structural features, including its silicate framework and distinct hydroxyl environments. Consequently, the FTIR spectral analysis not only validates the presence of a highly structured kaolinite material in the sample but also provides insight into the subtle structural variations that may influence its physico-chemical properties and subsequent industrial performance.

3.2. SEM and EDS result: The combined spectroscopic and microscopic analyses of the kaolin clay sample reveal a comprehensive picture of its structural and compositional attributes, which are critical for its industrial performance. The FTIR spectrum confirmed the presence of characteristic vibrational modes associated with the kaolinite structure specifically, the O–H stretching vibrations ($3620\text{--}3692\text{ cm}^{-1}$) indicative of multiple hydroxyl environments and the silicate framework vibrations ($640\text{--}1163\text{ cm}^{-1}$). These observations were further corroborated by SEM and EDS analyses, which provided a semi-quantitative elemental composition of the material as follows: Oxygen (59.9%), Silicon (17.3%), Aluminium (12.7%), Carbon (7.3%), Titanium (1.5%), and Iron (1.4%) as seen in figure 4.

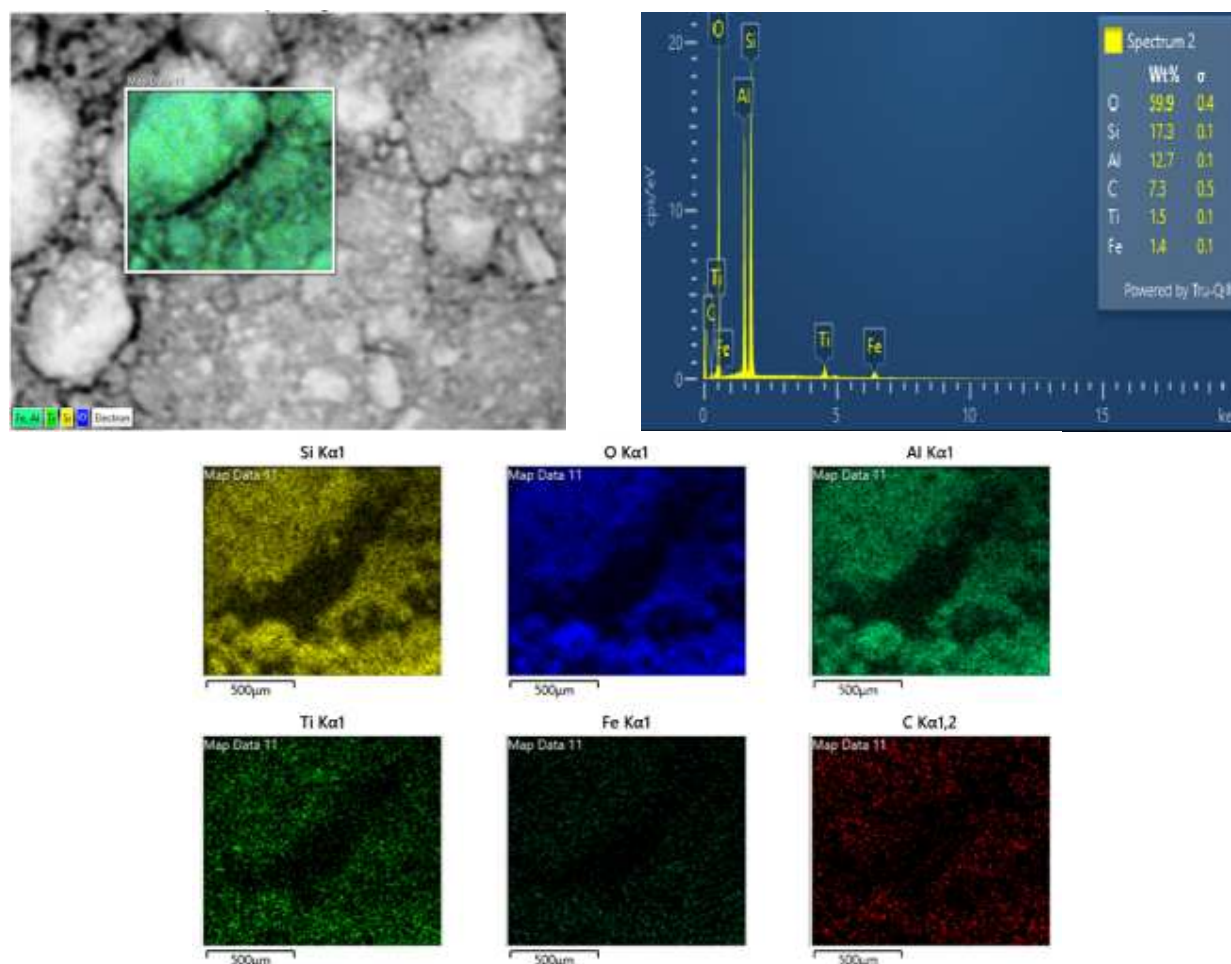


Fig. 4: SEM and EDS of Umuchieze kaolin clay

The dominance of oxygen, silicon, and aluminium in the EDS spectrum aligns well with the ideal kaolinite formula, $\text{Al}_2\text{Si}_2\text{O}_5(\text{OH})_4$, where a robust silicate network is expected. Although the measured weight percentages of silicon and aluminium are somewhat lower than the theoretical values, this discrepancy is typical of surface-sensitive techniques like EDS, which may underestimate light element contributions due to limitations in detector sensitivity and the potential influence of surface roughness or contamination [33]. The detection of carbon at 7.9% likely originates from surface contamination or residual organic matter, which is commonly observed in EDS analyses of clay minerals [34]. While this carbonaceous layer can potentially affect optical properties particularly brightness, which is a critical parameter for paper production its impact can be minimized through further purification or controlled processing.

Moreover, the trace amounts of titanium (1.5%) and iron (1.4%) suggest minor isomorphous substitutions or the presence of discrete impurity phases. In paper manufacturing, elevated levels of Fe and Ti can adversely affect the brightness and colour of the final product; however, their low concentrations in this sample imply that, with appropriate beneficiation, the clay can meet the stringent quality requirements for high-grade paper coatings. Conversely, in environmental remediation and catalysis applications, these trace elements might enhance the clay's reactivity by providing additional catalytic sites or modifying the surface charge distribution, thereby potentially improving adsorption efficiency and catalytic turnover. These results, along with FTIR data showing hydroxyl and silicate bands, suggest the Umuchieze kaolin sample is mainly kaolinite but with potential impurities.

- 3.3. TGA result: The TGA curve as shown in figure 5 exhibits an initial mass loss occurring between 32 °C and 100 °C, which is typically attributed to the removal of physically adsorbed water. This behaviour is consistent with the expected moisture content in clay minerals and supports the presence of loosely bound water molecules, as indirectly inferred from the FTIR absorption near 1600 cm^{-1} often associated with the bending vibration of water molecules.

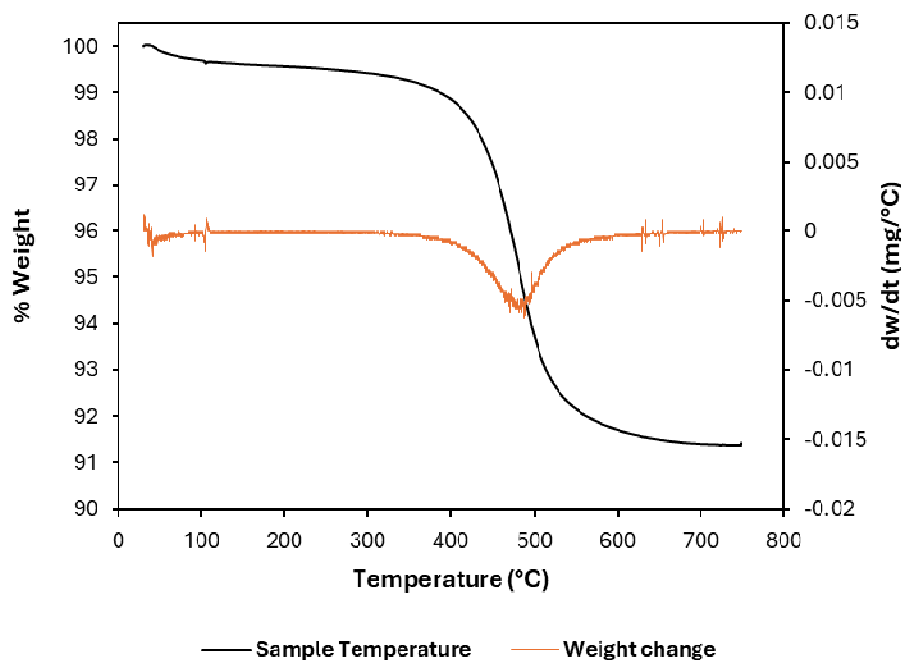


Fig. 5: TGA profile of Umuchieze kaolin clay

Following this initial phase, the sample shows negligible mass loss until the temperature reaches approximately 320 °C. This plateau indicates that the kaolin clay maintains its structural integrity in this temperature range, implying that no significant chemical transformations or loss of bound water occurs under moderate heating conditions. This stability is advantageous for industrial processes that require drying or moderate thermal treatment, such as in paper coating applications [7]. A pronounced mass loss is observed beginning at around 320 °C, which peaks at approximately 480 °C. This temperature range corresponds to the dehydroxylation process of the kaolinite structure the loss of structural hydroxyl groups (-OH) from the octahedral sheet. The FTIR data, which exhibited distinct O–H stretching bands in the high-frequency region ($3620\text{--}3692\text{ cm}^{-1}$), confirm the presence of these hydroxyl groups. The dehydroxylation peak at 480 °C is indicative of the transformation of kaolinite into metakaolin, a process well-documented in the literature Moore & Reynolds [35]. This transformation is critical for applications requiring thermally activated materials, such as catalysts or adsorbents, where changes in surface chemistry and reactivity can be exploited. After 480 °C, the TGA curve levels off, showing no further significant mass loss up to 800 °C. This thermal stability beyond the dehydroxylation stage implies that the resultant metakaolin phase is resistant to further thermal decomposition. Such stability is crucial for high-temperature industrial applications, including certain catalytic processes and ceramic formulations.

3.4. BET analysis: The measured BET surface area has a value of $\sim 23.76\text{ m}^2/\text{g}$ which is considered to be moderate and aligns well with the expected range for kaolinite clays that have not undergone extensive activation or delamination [36]. The average pore diameter of approximately 25 nm situates the material firmly within the mesoporous regime (2–50 nm) [37]. This mesoporosity is crucial for several industrial applications, as it facilitates the diffusion of reactants and products in catalytic and adsorption processes. The total pore volume of $0.1497\text{ cm}^3/\text{g}$ further supports the presence of an interconnected pore network, which can be particularly beneficial in processes such as environmental remediation, where the adsorption of contaminants relies on accessible pore channels.

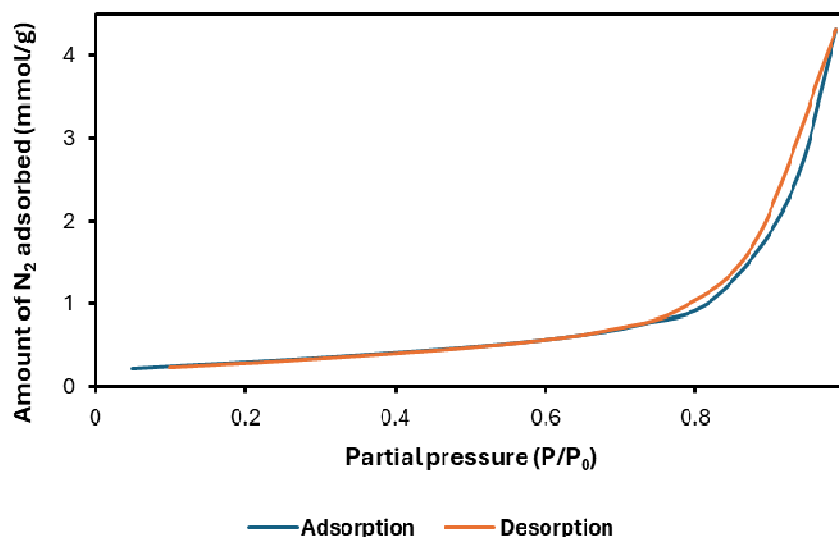


Fig. 6a: Liquid Nitrogen Physisorption Isotherm

The nitrogen physisorption isotherm of the kaolin sample, as depicted in figure 6a, exhibits characteristics of a Type V isotherm according to the IUPAC classification [38]. This classification is supported by the observation of 3 regions viz: Low-pressure Region ($P/P_0 < 0.4$) where the isotherm shows a slow initial uptake, which is consistent with weak physisorption interactions. Intermediate pressure region ($P/P_0 \sim 0.4$ to 0.8) where there is a steady increase in adsorption, likely due to multilayer adsorption rather than strong monolayer formation. Finally, high-pressure region ($P/P_0 > 0.8$) where a significant increase in adsorption occurs, indicative of capillary condensation in mesopores. The Type V isotherm is typically associated with materials where the adsorbate-adsorbent interactions are relatively weak, as seen in hydrophobized or poorly hydroxylated surfaces [14,39], certain modified clays [40], and some silica-based materials [41,42]. Additionally, the isotherm exhibits a noticeable hysteresis loop, which occurs due to the difference between the adsorption and desorption pathways. This loop is characterized by a steep desorption branch without a clear plateau at high relative pressures ($P/P_0 > 0.8$). It is commonly observed in aggregates of plate-like particles forming slit-shaped pores, which is typical of clays, layered silicates, and certain carbon-based materials [39]. Since kaolin has a layered structure, it is highly likely that the sample exhibits a Type H3 hysteresis loop, indicating mesoporosity due to slit-shaped voids between stacked kaolinite layers.

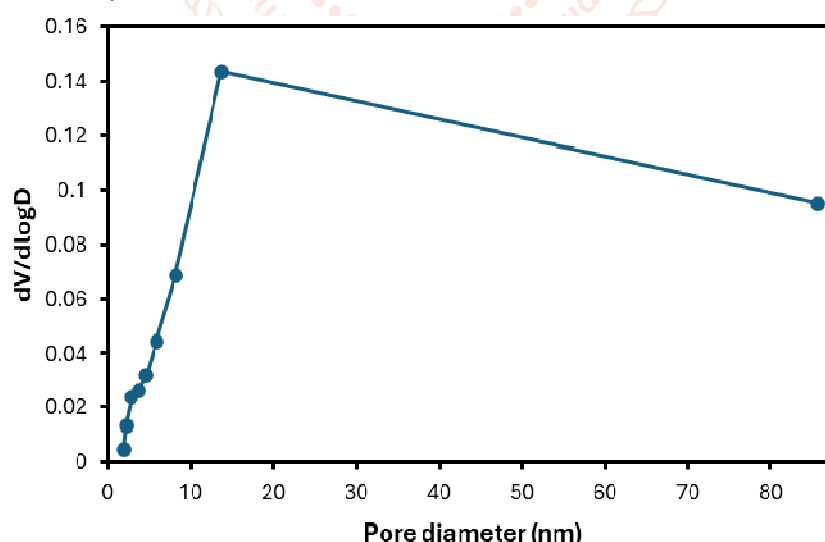


Fig. 6b: BJH desorption pore size distribution plot of the kaolin material

The BJH (Barrett-Joyner-Halenda) desorption pore size distribution plot depicted in figure 6b provides valuable insights into the pore structure of the kaolin material, particularly regarding mesoporosity and the nature of its porous network. From figure 6b, the peak pore diameter appears to be around 15–20 nm, indicating that the kaolin material predominantly contains mesopores (2–50 nm). A gradual decline in $dV/d\log D$ at larger pore diameters suggests the presence of some larger mesopores and possibly macropores (>50 nm). Furthermore, the steep initial increase followed by a gradual decline suggests a dominance of slit-shaped mesopores, which aligns

with the Type V isotherm and H3 hysteresis loop observed in the nitrogen adsorption-desorption isotherm. This type of pore network suggests limited pore interconnectivity, meaning that adsorption behaviour may be influenced by restricted diffusion pathways [38]. It is observed also that there is no significant peak at pore diameters below 2 nm, confirming that the material does not contain a substantial fraction of micropores. This aligns with the BET surface area result ($\sim 23.76 \text{ m}^2/\text{g}$), which is moderate and indicates the absence of highly microporous structures.

4. Suitability of Umuchieze kaolin for industrial applications

The comprehensive physicochemical analysis of the Umuchieze kaolin clay suggests its suitability for diverse industrial applications, including high-quality paper production, environmental remediation, adsorption processes, and catalytic systems. The structural integrity, surface chemistry, and thermal stability of the material play critical roles in determining its industrial relevance.

- 4.1. Paper production: The structural framework of the kaolin, as indicated by FTIR and SEM/EDS data, demonstrates sufficient mechanical stability for use in durable coatings. While the presence of trace impurities such as carbon, iron, and titanium may slightly reduce optical brightness, their low concentrations suggest that further refinement via flotation or acid leaching can enhance the material's brightness to meet industry standards.

Thermal analysis confirms that the kaolin maintains structural stability below 320°C , which is beneficial for its processing in paper manufacturing. The low abrasiveness of the material ensures minimal wear on production equipment, a key requirement in the paper industry. The moderate BET surface area is advantageous, as excessive surface reactivity could interfere with organic binder interactions, potentially affecting coating smoothness. The mesoporous structure enhances ink absorption and printability, making it a promising candidate as a filler or coating pigment. However, surface treatment may be required to improve dispersion and uniformity within papermaking slurries.

- 4.2. Environmental remediation and adsorption: The presence of surface hydroxyl groups, as confirmed by FTIR, provides reactive sites for pollutant adsorption. The elemental composition derived from SEM/EDS analysis indicates a stable kaolinite matrix capable of adsorbing heavy metals and organic contaminants. Additionally, the trace levels of iron and titanium oxides may contribute to enhanced surface reactivity under optimized conditions.

The mesoporous structure, with an average pore diameter of 25nm, facilitates the accessibility of

adsorption sites for larger organic pollutants and dyes. However, its efficiency in gas-phase adsorption may require surface modification. The material's moderate pore volume suggests a balance between adsorption capacity and mechanical stability, which is particularly beneficial in wastewater treatment applications. Post-dehydroxylation thermal treatment can enhance surface reactivity, increasing adsorption efficiency through additional active site formation.

- 4.3. Catalysis: The kaolinite structure provides a stable framework suitable for catalytic applications, particularly after thermal activation. The presence of hydroxyl groups ensures potential active sites for catalysis, while trace levels of iron and titanium may contribute to redox reactions. The TGA results confirm the transition from kaolinite to metakaolin at elevated temperatures, leading to the development of an enhanced porous structure that can be further functionalized with catalytic species.

The BET analysis indicates a moderate surface area with a well-defined mesoporous network, which supports its potential use as a catalyst support. The Type V isotherm and the corresponding mesoporous structure suggest that the material could be employed in diffusion-controlled catalytic processes. Functionalization strategies such as acid activation or transition metal doping may be necessary to optimize catalytic efficiency.

- 4.4. Ceramics and coatings: The pore size distribution and structural stability of the kaolin material suggest its suitability for ceramic applications. The controlled porosity contributes to mechanical strength and thermal stability, essential characteristics for high-performance ceramic components. The moderate surface area and stable mesoporous structure further enhance its applicability in coatings where thermal resistance and controlled permeability are required.

5. Conclusion

The comprehensive characterization of the Umuchieze kaolin clay confirms a well-developed kaolinite structure, as evidenced by FTIR analysis that revealed distinct silicate framework vibrations ($640\text{--}1163 \text{ cm}^{-1}$) and diverse O–H stretching bands

(3620–3691 cm⁻¹), indicative of a highly ordered and stable mineral. SEM and EDS analyses corroborated these findings by demonstrating a composition consistent with the ideal kaolinite formula dominated by oxygen, silicon, and aluminium with trace levels of carbon, titanium, and iron that, with proper beneficiation, are unlikely to hinder industrial performance. Thermogravimetric analysis further established the material's thermal stability, showing initial mass loss due to adsorbed water up to 100°C, stability up to 320°C, and dehydroxylation between 320°C and 480°C, after which a thermally stable metakaolin phase is formed. Additionally, BET analysis revealed a moderate surface area (~23.76 m²/g), a total pore volume of 0.1497 cm³/g, and an average pore diameter of approximately 25 nm, with a Type V isotherm and H3 hysteresis loop indicating mesoporosity and slit-shaped pores. Collectively, these findings demonstrate the material's robust structural integrity and versatile textural properties, underscoring its potential for high-quality paper production, efficient environmental remediation, effective adsorption processes, and catalytic applications in oil and gas processes. Further studies on surface functionalization, pore engineering, and structural modifications will significantly enhance the industrial applications of Umuchieze kaolin. By tailoring its properties to specific industry needs such as high brightness in papermaking, selective adsorption in wastewater treatment, enhanced porosity for gas separation, and catalytic activity in oil refining Umuchieze mined kaolin can be optimized for greater economic and environmental benefits.

Acknowledgements

Briggs Martins Onyinyechukwu Ogunedo expresses gratitude to the Petroleum Technology Development Fund (PTDF), Nigeria, for the doctoral study scholarship (Award Number: PTDF/ED/OSS/PHD/BOO/1710/20) and to Imo State University, Owerri, Nigeria, for their support.

Funding

No specific grant was received for this research from funding agencies in the public, commercial, or non-for-profit sectors.

Declarations

Conflict of interests: The authors affirm that there are no conflicts of interest in this research work.

Ethics Approval

Not applicable.

Informed consent for Publication

The authors have unanimously agreed that this manuscript be sent for possible publication.

Consent to Participate declaration

Not applicable

Clinical trial number

Not applicable

Data availability declaration

The datasets generated during and/or analysed during the current study are available from the corresponding author on reasonable request.

References

- [1] I.M. Savic Gajic, S.T. Stojiljkovic, I.M. Savic, Industrial application of clays and clay minerals, Nova Science Publishers. Inc., New York, 2014. www.gajicassociates.com.
- [2] S. Khan, S. Ajmal, T. Hussain, M.U. Rahman, Clay-based materials for enhanced water treatment: adsorption mechanisms, challenges, and future directions, Journal of Umm Al-Qura University for Applied Sciences (2023). <https://doi.org/10.1007/s43994-023-00083-0>.
- [3] W.T. Sibhat, H.S. Ayele, M. Atlabachew, K.S. Mohammed, B.A. Aragaw, B. Abebaw, D.T. Ayele, Effect of Ethiopian kaolin treatment on the performance of adsorptive removal of methylene blue dye, Results Chem 13 (2025). <https://doi.org/10.1016/j.rechem.2025.102027>.
- [4] B. Fashina, Y. Deng, STACKING DISORDER AND REACTIVITY OF KAOLINITES, Clays Clay Miner 69 (2021) 354–365. <https://doi.org/10.1007/s42860-021-00132-x>.
- [5] S.C. Aboudi Mana, M.M. Hanafiah, A.J.K. Chowdhury, Environmental characteristics of clay and clay-based minerals, Geology, Ecology, and Landscapes 1 (2017) 155–161. <https://doi.org/10.1080/24749508.2017.1361128>.
- [6] S. Mustapha, M.M. Ndamitso, A.S. Abdulkareem, J.O. Tijani, A.K. Mohammed, D.T. Shuaib, Potential of using kaolin as a natural adsorbent for the removal of pollutants from tannery wastewater, Heliyon 5 (2019). <https://doi.org/10.1016/j.heliyon.2019.e02923>.
- [7] A.G. Adeniyi, K.O. Iwuzor, E.C. Emenike, Material Development Potential of Nigeria's Kaolin, Chemistry Africa 6 (2023) 1709–1725. <https://doi.org/10.1007/s42250-023-00642-2>.
- [8] M.S.H. Badr, S. Yuan, J. Dong, H. El-Shall, Y.A. Bermudez, D.C. Ortega, J.E. Lopez-Rendon, B.M. Moudgil, The properties of Kaolin from different locations and their impact on casting rate, KONA Powder and Particle

- Journal 38 (2021) 251–259.
<https://doi.org/10.14356/kona.2021002>.
- [9] S. Kaufhold, M. Hein, R. Dohrmann, K. Ufer, Quantification of the mineralogical composition of clays using FTIR spectroscopy, *Vib Spectrosc* 59 (2012) 29–39.
<https://doi.org/10.1016/j.vibspec.2011.12.012>.
- [10] G. Jozanikohan, M.N. Abarghooei, The Fourier transform infrared spectroscopy (FTIR) analysis for the clay mineralogy studies in a clastic reservoir, *J Pet Explor Prod Technol* 12 (2022) 2093–2106.
<https://doi.org/10.1007/s13202-021-01449-y>.
- [11] A. Yunusa, H. Hong, A. Salim, T. Amam, C. Liu, Y. Xu, X. Zuo, Z. Li, Mineralogical Characterization and Geochemical Signatures of Supergene Kaolinitic Clay Deposits: Insight of Ropp Complex Kaolins, Northcentral Nigeria, *Minerals* 14 (2024) 869.
<https://doi.org/10.3390/min14090869>.
- [12] K. AZIZI, J. MAISSARA, M. ELMAHI CHBIHI, Y. NAIMI, Thermal Transformation of Kaolinite Clays: Analyzing Dehydroxylation and Amorphization for Improved Pozzolanic Performance, *International Journal of Chemical and Biochemical Sciences* 25 (2024).
<https://doi.org/10.62877/127-ijcbs-24-25-19-127>.
- [13] Nigerian Geological Survey Agency, Mineral Resources Map of Nigeria 2023, (2023).
http://ngsa.gov.ng/wp-content/uploads/2023/08/Mineral_Resources_Map_of_Nigeria_2023.pdf (accessed February 3, 2025).
- [14] F.I. Adeniyi, M.B. Ogundiran, T. Hemalatha, B.B. Hanumantrai, Characterization of raw and thermally treated Nigerian kaolinite-containing clays using instrumental techniques, *SN Appl Sci* 2 (2020). <https://doi.org/10.1007/s42452-020-2610-x>.
- [15] A. Mamudu, M. Emetere, D. Okocha, S. Taiwo, F. Ishola, F. Elehinafe, E. Okoro, Parametric investigation of indigenous Nigeria mineral clay (Kaolin and Bentonite) as a filler in the Fluid Catalytic Cracking Unit (FCCU) of a petroleum refinery, *Alexandria Engineering Journal* 59 (2020) 5207–5217.
<https://doi.org/10.1016/j.aej.2020.09.050>.
- [16] U. Omeiza Aroke, U. Aliyu El-Nafaty, O. Osha, A.U. O, E.-N.U. A, O.O. A, Properties and characterization of kaolin clay from Alkalari, north-eastern Nigeria *International Journal of Emerging Technology and Advanced Engineering Properties and Characterization of Kaolin Clay from Alkalari, North-Eastern Nigeria*, 2008.
<https://www.researchgate.net/publication/281378945>.
- [17] B.C. Chukwudi, Characterization and Evaluation of the Refractory Properties of Nsu Clay Deposit in Imo State Nigeria, *Pacific Journal of Science and Technology* 9 (2008) 487–494.
<http://www.akamaiuniversity.us/PJST.htm>.
- [18] E. Ameh, A. Ogbodo Agbo, C. Chidi Nwogbu, A.A. O, SUITABILITY OF EHA-NDIAGU CLAYS FOR THE PRODUCTION OF LABORATORY CRUCIBLES, 2018.
<http://esrjournal.com>.
- [19] B.S. Badmus, O.B. Olatinsu, Geophysical evaluation and chemical analysis of kaolin clay deposit of Lakiri village, southwestern Nigeria, 2009. <http://www.academicjournals.org/IJPS>.
- [20] B. Ali, Z.T. Dikko, Geochemical And Geological Characterisation Of Kaolinite Deposits Around Kaoje, Kebbi State, Nigeria, *INTERNATIONAL JOURNAL OF SCIENTIFIC & TECHNOLOGY RESEARCH* 4 (2015). www.ijstr.org.
- [21] G. Paul Ojo, C.J. Egbuachor Belushi, K. Nwozor, G. Ojo, U. Igbokwe, C. Egbuachor, K. Nwozor, Geotechnical Properties and Geochemical Composition of Kaolin Deposits in Parts of Ifon, Southwestern Nigeria Ugochukwu G Igbokwe Geotechnical Properties and Geochemical Composition of Kaolin Deposits in Parts of Ifon, Southwestern Nigeria, (2017) 15–24. www.ajer.org.
- [22] V. Dorawa, C. Emmanuel, E. Onochie Nwabineli, J. Ewaoche, Geochemical and Mineralogical Studies of Clay Deposits in Avutu Obowo Study Area Southeastern Nigeria for Industrial Uses, *International Journal of Research Publication and Reviews* 5 (2024) 1147–1158. www.ijrpr.com.
- [23] A.G. Olaremu, Physico-Chemical Characterization of Akoko Mined Kaolin Clay, *Journal of Minerals and Materials Characterization and Engineering* 03 (2015) 353–361.
<https://doi.org/10.4236/jmmce.2015.35038>.
- [24] Thaddeus. C. Azubuike, Paulinus. N. Nnabo, Norbert Okechinyere Osonwa, Chukwuemeka Emmanuel Odoala, Emma Onochie Nwabineli,

- Victor Dorawa Koreyo, Mineralogical, geochemical and physical properties assessment of clay deposits in Umuoke Obowo Southeastern Nigeria for industrial applications, *World Journal of Advanced Research and Reviews* 21 (2024) 533–545. <https://doi.org/10.30574/wjarr.2024.21.3.0699>.
- [25] J.O. Osumaje, E. Daniel, K.M. Lawal, Application of geophysical method to delineate Kaolin deposit at Kankara, Northwestern Nigeria, *Dutse Journal of Pure and Applied Sciences* 7 (2022). <https://doi.org/10.4314/dujopas.v7i4b.5>.
- [26] A.J. Abegunde, A.O. Adebayo, P.O. Ajewole, COMPARATIVE STUDY OF KAOLIN DEPOSITS IN SOUTHWESTERN NIGERIA, *Journal of Engineering and Earth Sciences* 17 (2024) 102–114.
- [27] G.O. Ihekwe, J.N. Shondo, K.I. Orisekeh, G.M. Kalu-Uka, I.C. Nwuzor, A.P. Onwualu, Characterization of certain Nigerian clay minerals for water purification and other industrial applications, *Heliyon* 6 (2020). <https://doi.org/10.1016/j.heliyon.2020.e03783>.
- [28] B.O. Omang, E.A. Kudamnya, A.O. Owolabi, J. Odey, E.U. Aniwetalu, T.A. Ako, Characterization of Kaolin Deposits in Okpella and Environs, Southern Nigeria, *International Journal of Geosciences* 10 (2019) 317–327. <https://doi.org/10.4236/ijg.2019.103018>.
- [29] J. Madejová, FTIR techniques in clay mineral studies, n.d.
- [30] E. Plevova, L. Vaculikova, V. Valovicova, Thermal analysis and FT-IR spectroscopy of synthetic clay mineral mixtures, *J Therm Anal Calorim* 142 (2020) 507–518. <https://doi.org/10.1007/s10973-020-09527-9>.
- [31] P. Djomgoue, D. Njopwouo, FT-IR Spectroscopy Applied for Surface Clays Characterization, *J Surf Eng Mater Adv Technol* 03 (2013) 275–282. <https://doi.org/10.4236/jsemt.2013.34037>.
- [32] V.C. Khang, M. V. Korovkin, L.G. Ananyeva, Identification of clay minerals in reservoir rocks by FTIR spectroscopy, in: *IOP Conf Ser Earth Environ Sci*, Institute of Physics Publishing, 2016. <https://doi.org/10.1088/1755-1315/43/1/012004>.
- [33] M. Morita, Scanning Electron Microscope Energy Dispersive X-Ray Spectrometry, in: *T.S.S.S. of Japan (Ed.), Compendium of Surface and Interface Analysis*, Springer Singapore, Singapore, 2018: pp. 557–561. https://doi.org/10.1007/978-981-10-6156-1_90.
- [34] P. Jacquemot, J.C. Viennet, S. Bernard, C. Le Guillou, B. Rigaud, L. Delbes, T. Georgelin, M. Jaber, The degradation of organic compounds impacts the crystallization of clay minerals and vice versa, *Sci Rep* 9 (2019). <https://doi.org/10.1038/s41598-019-56756-6>.
- [35] C. V. Jeans, M OORE, D. M. & R EYNOLDS, R. C., Jr. 1997. *X-Ray Diffraction and the Identification and Analysis of Clay Minerals*, 2nd ed. xviii + 378 pp. Oxford, New York: Oxford University Press. Price £27.95 (spiral-bound paperback). ISBN 0 19 508713 5., *Geol Mag* 135 (1998) 819–842. <https://doi.org/10.1017/s0016756898501501>.
- [36] R. Deju, A. Cucos, M. Mincu, C. Tuca, THERMAL CHARACTERIZATION OF KAOLINITIC CLAY, 2021.
- [37] Fundamental Factors for Designing Adsorbent, in: *Adsorbents: Fundamentals and Applications*, John Wiley & Sons, Ltd, 2003: pp. 8–16. <https://doi.org/https://doi.org/10.1002/047144409X.ch2>.
- [38] M. Thommes, K. Kaneko, A. V. Neimark, J.P. Olivier, F. Rodriguez-Reinoso, J. Rouquerol, K.S.W. Sing, Physisorption of gases, with special reference to the evaluation of surface area and pore size distribution (IUPAC Technical Report), *Pure and Applied Chemistry* 87 (2015) 1051–1069. <https://doi.org/10.1515/pac-2014-1117>.
- [39] K.S.W. Sing, INTERNATIONAL UNION OF PURE AND APPLIED CHEMISTRY PHYSICAL CHEMISTRY DIVISION COMMISSION ON COLLOID AND SURFACE CHEMISTRY INCLUDING CATALYSIS SUBCOMMITTEE ON REPORTING GAS ADSORPTION DATA* REPORTING PHYSISORPTION DATA FOR GAS/SOLID SYSTEMS with Special Reference to the Determination of Surface Area and Porosity, 1982.
- [40] O. Seitnazarova, A. Kalbaev, N. Mamataliev, A. Abdikamalova, N. Najimova, STRUCTURAL FEATURES OF MONTMORILLONITE-SURFACTANT SYSTEMS: INFLUENCE OF SURFACTANT PACKING DENSITY AND MONTMORILLONITE SURFACE NATURE,

- Journal of Chemical Technology and Metallurgy 60 (2025) 43–62.
<https://doi.org/10.59957/jctm.v60.i1.2025.5>.
- [41] M. Thommes, K.A. Cychosz, Physical adsorption characterization of nanoporous materials: Progress and challenges, Adsorption 20 (2014) 233–250.
<https://doi.org/10.1007/s10450-014-9606-z>.
- [42] P.I. Ravikovitch, A. V. Neimark, Experimental confirmation of different mechanisms of evaporation from ink-bottle type pores: Equilibrium, pore blocking, and cavitation, Langmuir 18 (2002) 9830–9837.
<https://doi.org/10.1021/la026140z>.

